

Geologica Acta: an international earth science journal

ISSN: 1695-6133

geologica-acta@ictja.csic.es

Universitat de Barcelona España

Errandonea-Martin, J.; Carracedo-Sánchez, M.; Sarrionandia, F.; Santos Zalduegui, J. F.; García de Madinabeitia, S.; Gil-Ibarguchi, J. I.

The late-Variscan peraluminous Valdepeñas pluton (southern Central Iberian Zone)
Geologica Acta: an international earth science journal, vol. 15, núm. 4, diciembre, 2017,
pp. 361-378

Universitat de Barcelona Barcelona, España

Available in: http://www.redalyc.org/articulo.oa?id=50553843008



Complete issue

More information about this article

Journal's homepage in redalyc.org



© J. Errandonea-Martin, M. Carracedo-Sánchez, F. Sarrionandia, J. F. Santos Zalduegui, S. García de Madinabeitia, J. I. Gil-Ibarquchi, 2017 CC BY-SA

The late-Variscan peraluminous Valdepeñas pluton (southern Central Iberian Zone)

J. ERRANDONEA-MARTIN¹ M. CARRACEDO-SÁNCHEZ¹ F. SARRIONANDIA² J. F. SANTOS ZALDUEGUI¹ S. GARCÍA DE MADINABEITIA¹ J. I. GIL-IBARGUCHI¹

¹Dep. of Mineralogy and Petrology, Faculty of Science and Technology, University of the Basque Country UPV/EHU

C/ Sarriena s/n, 48940 Leioa, Spain

²Dep. of Geodynamics, Faculty of Pharmacy, University of the Basque Country UPV/EHU 01006 Vitoria, Spain

$^{+}$ ABSTRACT $^{+}$

The Valdepeñas pluton is the easternmost outcrop of the Cáceres-Valdepeñas magmatic alignment (southern Central Iberian Zone). This massif is constituted by a cordierite-bearing porphyritic monzogranite and may be grouped within the so-called "Serie Mixta" granitoids. The Valdepeñas monzogranite is of magnesian $[FeO_t/(FeO_t+MgO)\sim0.76]$, alkali-calcic $[(Na_2O+K_2O)-CaO=7.8-8.5]$ and peraluminous (A/CNK=1.14-1.20)composition. Multielemental- and REE-normalized patterns are comparable to those of similar rocks in the Nisa-Alburquerque-Los Pedroches magmatic alignment, and slightly differ from those of the Montes de Toledo batholith, both in the southern Central Iberian Zone. The U-Pb zircon age of 303±3Ma is consistent with the late-orogenic character of the intrusion and is in accordance with most of the granitic peraluminous intrusions in the southern Central Iberian Zone. ⁸⁶Sr/⁸⁷Sr_{300Ma} ratios (0.707424–0.711253), εNd_{300Ma} values (-5.53 to -6.68) and whole-rock major and trace element compositions of the studied rocks, suggest that the parental magma of the Valdepeñas monzogranite could derive from a crustal metaigneous source. The U-Pb ages (552-650Ma) of inherited zircon cores found in Valdepeñas monzogranite samples match those often found in Lower Paleozoic metavolcanics and granitic orthogneisses of Central Iberia and, furthermore, point to Upper Neoproterozoic metaigneous basement rocks as possible protoliths at the magma source. Based on the solubility of monazite in peraluminous melts, the estimated emplacement temperature of the studied monzogranite is 742–762°C. The results obtained in this work would contribute to a better understanding of the origin of the "Serie Mixta" granitoids.

KEYWORDS

Peraluminous. Monzogranite. Metaigneous source. Central Iberian Zone. Valdepeñas.

INTRODUCTION

The Central Iberian Zone (CIZ; Iberian Massif) records an important late-Variscan crustal tectonomagmatic event, as reflected by several large granitic intrusions dated in this area (e.g. Bea et al., 2003;

Carracedo et al., 2009; Gutiérrez-Alonso et al., 2011; Merino Martínez et al., 2014). This magmatism has been related to crust-derived melts (e.g. Capdevila et al., 1973; Corretgé, 1983; Corretgé, 1985; González Menéndez, 1998; Villaseca et al., 1998b; Bea et al., 1999; Alonso Olazabal, 2001; Merino Martínez et al.,

2014), synchronous or later than the main deformational and metamorphic events (López Plaza and Martínez Catalán, 1987; González Menéndez, 1998; Alonso Olazabal, 2001). Besides that, several granitoids point to a variable contribution of mantle-derived components in the genesis of the crustal source melts (e.g. Castro et al., 1999; Alonso Olazabal, 2001; García-Moreno, 2004). Traditionally, in the southern areas of the CIZ the intrusive massifs have been grouped into three main magmatic alignments known, from South to North, as: i) Nisa-Alburquerque-Los Pedroches, ii) Cáceres-Valdepeñas, and iii) Montes de Toledo (e.g. Aparicio et al., 1977; Fig. 1A).

The southernmost alignment, Nisa-Alburquerque-Los Pedroches, is defined by late- Variscan intrusions arranged along ~400km parallel to the main Variscan tectonic structures (N120E trend). Except for the calcalkaline granodiorites of the Los Pedroches batholith, these intrusions are constituted by Ca-poor and P-rich peraluminous granites, with low Sr isotopic initial relations and emplacement ages of 304–314Ma (García de Madinabeitia *et al.*, 2003; Carracedo *et al.*, 2009; Solá *et al.*, 2009; Gutiérrez-Alonso *et al.*, 2011). These massifs were emplaced in the upper crust at ~2.5–3.5kbar and

temperatures of 640–800°C (*e.g.* González Menéndez, 1998; Alonso Olazabal, 2001). According to isotope geochemical data, the intrusions would be derived from metasedimentary and metaigneous sources (*e.g.* González Menéndez, 1998; Alonso Olazabal, 2001).

northernmost alignment (~200km long) corresponds mainly to the Montes de Toledo batholith, which includes ~20 granitoid intrusions aligned in N100E direction. They correspond to late-Variscan leucogranites and monzogranites with a variable peraluminous character that can reach up to extremely high values of peraluminousity. These granitoids stand out by their marked phosphorous-rich character (up to 0.9 wt.% P₂O₅; Bea et al., 1992; Villaseca et al., 2008). These intrusions' initial Sr isotope values are also variable but, in several cases, they are relatively high (~ 0.722) and their emplacement ages are 297-316Ma (Merino Martínez et al., 2014). According to Bea et al. (1994) and Merino Martínez et al. (2014), these melts were emplaced in the upper crust (1–2kbar), under a relatively wide range of temperatures (630-880°C). Inferred sources were essentially metasedimentary (anatectic melts), with a minor contribution of metaigneous or hybrid (metasedimentary and metaigneous) sources

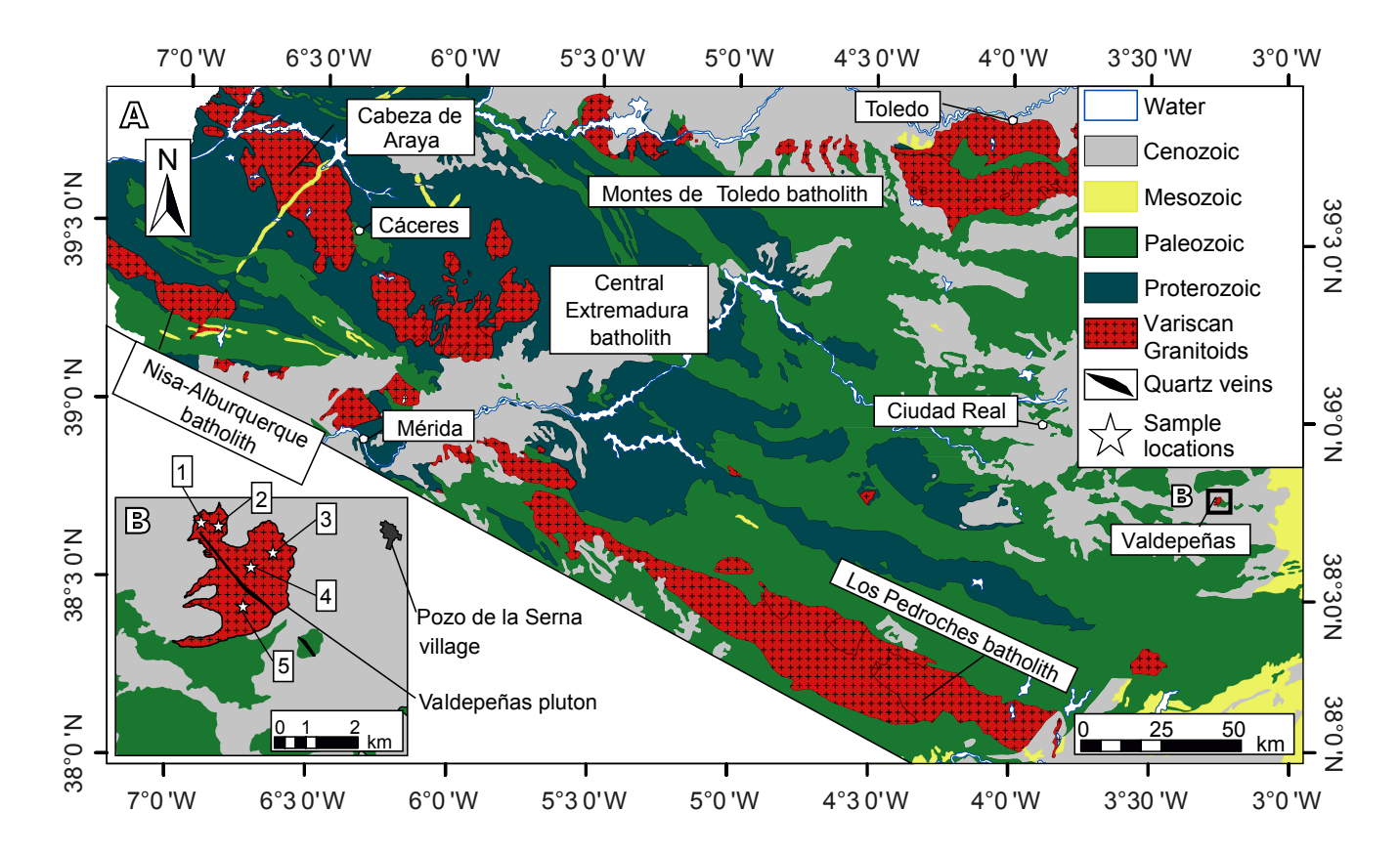


FIGURE 1. A) Geological map of the southern Central Iberian Zone showing the main Variscan magmatic alignments (modified after Caride de Liñán, 1994). B) Geological sketch of the studied area (see Figure 1A for location).

(Andonaegui, 1990; Barbero *et al.*, 1990; Villaseca *et al.*, 1998b; Barbero and Villaseca, 2004; Villaseca *et al.*, 2008; Merino Martínez *et al.*, 2014).

The Cáceres-Valdepeñas alignment is located between the aforementioned two magmatic alignments and extends along ~350km in N100-120E direction (Fig. 1A). Due to its size, the so-called Central Extremadura batholith (sensu Castro, 1986; Castro et al., 1999; Castro et al., 2002), which includes the large Cabeza de Araya massif (sometimes regarded as a batholith itself, e.g. Corretgé et al., 1985) and a few accompanying minor intrusions (Plasenzuela, Trujillo, etc.), represents the main component of this alignment, circumscribing most of the intrusions of the region. This batholith is mainly constituted by a peculiar type of granitoids, known as "Serie Mixta" (mixed series) granites or "Cabeza de Araya type" (e.g. Corretgé, 1971), which corresponds to alkali-, calcalkaline granites with a marked peraluminous character (cordierite ± Al₂SiO₅ ± garnet-bearing). They exhibit low Ca values and high P contents (Corretgé et al., 1985; Castro et al., 2002; Corretgé et al., 2004). These granitoids show intermediate characteristics between magmas derived from sedimentary-rich sources (peraluminous leucogranites) and peraluminous granodiorites derived from metaigneous sources. These magmas would be emplaced in the upper crust at ~3-4kbar and 700-850°C (Garcia-Moreno, 2004; Garcia-Moreno *et al.*, 2007). Though metasedimentary rocks are in the beginning a highly plausible source for the origin of these melts, the contribution of protoliths with mantle signature seems more than likely (e.g. Castro et al., 1999; García-Moreno, 2004).

The easternmost intrusion included in the Cáceres-Valdepeñas alignment is the here studied Valdepeñas pluton, also known as Pozo de la Serna pluton in the regional literature. This small granitic intrusion crops out next to the CM-412 road (kilometric points 46 to 48) that connects the villages of Valdepeñas and Pozo de la Serna (Ciudad Real province, Fig. 1A; B). Perhaps because of its small size, no detailed petrological characterization of this massif has been done before. This contribution presents the petrography, mineral geochemistry, conventional and isotope (Rb-Sr; Sm-Nd) whole-rock geochemistry, and zircon U-Th-Pb geochronology of this pluton. Based on these data, we discuss the magma sources involved in the genesis of this pluton in the framework of the petrogenetic models proposed for the late-Variscan magmatism of the southern CIZ (SW Iberian Massif). The conclusions of the study should be of special interest for future studies on the origin of the granitoids grouped in the so-called mixed series ("Serie Mixta") granites.

GEOLOGICAL CONTEXT AND FIELD CHARACTERISTICS

The regional basement of the Valdepeñas pluton is constituted by the Schist and Greywacke Complex (Neoproterozoic-Lower Cambrian; Carrington da Costa 1950; Rodríguez Alonso *et al.*, 2004), discordantly covered by a Paleozoic (Ordovician-Carboniferous) metasedimentary sequence, structured in N120E trending large Variscan folds (Martínez Poyatos *et al.*, 2004). In some places, the basement is discordantly overlaid by Cenozoic sedimentary sequences.

The Valdepeñas pluton crops out in a nearly circular small area (~3km²) surrounded by the Cenozoic cover, which impedes the observation of intrusion relations with the metasedimentary units (Fig. 1A). Nonetheless, despite its apparently small size at outcrop scale, gravimetric data indicate that this intrusion could be ~10km wide and <9km deep (Bergamín and De Vicente, 1985). The pluton is constituted by a cordierite-bearing porphyritic monzogranite, being noteworthy the absence of mafic microgranular enclaves (MME). The studied monzogranitic rocks are massive and homophanous. Their porphyritic character is defined by the presence of alkali feldspar phenocrysts (up to 4cm long), which are included in a biotite-bearing medium- to coarse-size granitic groundmass. Abundant globular quartz aggregates (up to 1.2cm long) and cordierite (0.8cm long) stand out in the groundmass (Fig. 2A; B).

The porphyritic monzogranite appears in some places hydrothermally altered. Altered zones locate close to, or appear cut by, N160E trending quartz veins up to 45cm thick. The veins are parallel to the main joint system observed in the monzogranite mass. This system (N160E) is arranged in 60–70cm wide bands constituted by several parallel joints separated 10–15cm.

METHODS

Five representative samples of the Valdepeñas pluton have been studied in detail using different laboratory procedures. The field mesoscopic petrographic characterization was completed by digital studies of scanned images obtained from hand specimen cuttings. The petrographic observations in thin sections were done by a polarizing microscope Leica DM LP model fitted with a CCD camera. The proportions of rock components were obtained by point-count modal analyses. Polished thin sections were studied by electron microprobe techniques for mineral geochemical characterization at the University of Oviedo using a Cameca SX100 instrument. Operating conditions of the microprobe were:

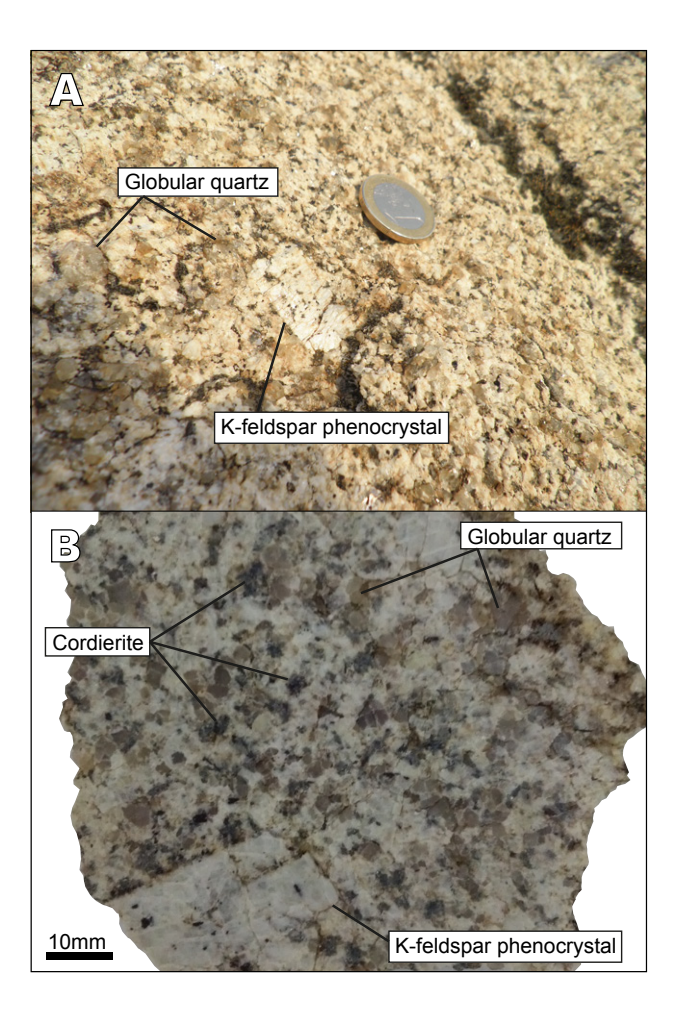


FIGURE 2. A) Field textural characteristics of the Valdepeñas cordierite-bearing porphyritic monzogranite. B) Scanned section of a sample of the studied monzogranite, where it stands out the relative abundance of globular quartz aggregates and cordierite prisms.

10s counting time (peak), ~10nA beam current and 15kV accelerating voltage. Calibration was against BRGM (French Geological Survey) standard minerals and the ZAF correction procedure was used. Both elemental bulk rock and isotopic analyses were performed at the Geochronology and Isotope Geochemistry SGIker-Facility of the UPV/EHU. Elemental analyses were done by inductively coupled plasma mass spectrometry (ICP-MS; Thermo Fisher XSeries 2) after sample fusion with LiBO₂ and subsequent dissolution in diluted HNO₃:HF acid mixture. The precision for all analytes is generally <2% (always <4%; cf. García de Madinabeitia et al., 2008 for additional details on the analytical procedure). Sm and Nd concentrations were determined by isotope dilution thermal ionization mass spectrometry (TIMS, Finnigan MAT262) after sample dissolution in closed Savillex PFA vessels using a mixed 149Sm/150Nd tracer. The precision typically achieved on ¹⁴⁷Sm/¹⁴⁴Nd ratios and Sm and Nd concentrations is 0.5% at a 95% confidence level. In the same sample solution obtained for Sm and Nd determination, Sr isotopic ratios were determined using multicollection inductively coupled plasma mass spectrometry (MC-ICP-MS, Neptune, Thermo Fisher Scientific). Rb and Sr concentrations were obtained in the bulk rock analysis, and 87Rb/86Sr ratios were calculated from these data and the ⁸⁷Sr/⁸⁶Sr measured ratios. The precision for concentrations and Rb/Sr ratios is typically 2% at a 95% confidence level. U-Th-Pb isotope measurements of zircon grains were conducted by LA-ICP-MS. The samples were ablated with a 213nm Nd:YAG based laser ablation (LA) system (NewWave Research) coupled to a quadrupolebased ICP-MS (Thermo XSeries 2). Spot diameters of 30µm associated to repetition rates of 10Hz and laser fluence at the target of ~2.5J/cm² were used. The signals of ²⁰²Hg, ²⁰⁴(Pb + Hg), ²⁰⁶Pb, ²⁰⁷Pb, ²⁰⁸Pb, ²³²Th, ²³⁵U and ²³⁸U masses were determined. The occurrence of common Pb in the samples was monitored by the evolution of ²⁰⁴(Pb + Hg) signal intensity, and those analyses with common Pb were rejected. Data reduction was carried out with Iolite v. 3 (Paton et al., 2011) and VizualAge (Petrus and Kamber, 2012), using GJ-1 zircon standard (Jackson et al., 2004) for calibration, and Plešovice zircon (Sláma et al., 2008) as a secondary standard. Percentage concordance was calculated as [(206Pb/238U age) / (207Pb/206Pb age)] × 100 (Meinhold et al., 2010) (cf. Ábalos et al., 2012 for additional details on the LA-ICP-MS analytical procedure).

PETROGRAPHY AND MINERAL GEOCHEMISTRY

The cordierite-bearing porphyritic monzogranite of Valdepeñas exhibits an hypidiomorphic porphyritic texture defined by alkali feldspar phenocrystals included into a medium- to coarse-size groundmass constituted by quartz, plagioclase, alkali feldspar, biotite, cordierite, apatite, zircon, monazite, muscovite and opaque minerals (Fig. 3A).

Alkali feldspar phenocrystals are up to 4cm long and subhedral. They often exhibit perthitic exsolutions, and Frasl inclusions of biotite, plagioclase, apatite and muscovite (Fig. 3A). Plagioclase (1-5mm; 30-40 vol.%) is idiomorphic, and alteration to sericite is observed at crystal cores. Quartz (25–35 vol.%) appears as xenomorphic globular crystals, generally defining glomeroporphyritic aggregates (Fig. 2A; B). Biotite (1-2mm; 3-8 vol.%) is idiomorphic, can be partially or totally transformed to secondary muscovite (Fig. 3B), and frequently contains inclusions of apatite, monazite and zircon (Fig. 3B; C). Cordierite (≤10mm; 3–6 vol.%) appears often completely altered to pinite, muscovite and biotite (Fig. 3D). Muscovite appears mainly as alteration of cordierite and biotite, but also as idiomorphic primary crystal. Since muscovite can replace completely biotite, sometimes it is not possible to discriminate between primary and secondary muscovite. Apatite may occur as idiomorphic prisms ($100\text{--}400\mu\text{m}$) included into biotite and alkali feldspar, or as isolated crystals in the groundmass (Fig. 3C).

The composition of alkali feldspar phenocrystals is the same as the subidio- xenomorphic (8–9mm; 15–30 vol.%) ones from the groundmass (Or₈₉₋₉₈; Fig. 4A). Plagioclase is compositionally zoned, with variable compositions for the cores (up to An₅₉) and rims (An₀₂₋₂₈; Fig. 4A). The biotite is primary (Fig. 4B) and compositionally rich in Al (Fig. 4C; D), though they plot in the calc-alkaline field of the FeO_t–MgO–Al₂O₃ diagram (Rossi and Chevremont, 1987). Cordierite is magmatic (Fig. 4E) and shows some variations in MgO (4.82–8.06 wt.%) and FeO (7.90%–11.93 wt.%). Muscovite with primary features is scarce and has a not very different composition from the one formed by the alteration of biotite (Fig. 4F).

WHOLE-ROCK GEOCHEMISTRY

Five samples were selected for whole-rock geochemical characterization (Table 1). The results

obtained indicate that variations in major element concentrations are practically negligible. Granitic rocks of the Valdepeñas pluton are compositionally homogeneous (Al $_2$ O $_3$ =14.50–14.92 wt.%; K $_2$ O+Na $_2$ O=8.36–9.23 wt.%), acid (SiO $_2$ =71.56–72.87 wt.%), low-Ca (CaO=0.66–0.72 wt.%) and phosphorous-rich (P $_2$ O $_5$ =0.29–0.30 wt.%), with low total Fe $_2$ O $_3$ t+MgO+TiO $_2$ +MnO content (2.02–2.33 wt.%).

These rocks plot in the sub-alkaline granite field of the TAS (Wilson, 1989) and Ab–An–Or (O'Connor, 1965) diagrams. Geochemically are peraluminous (A/CNK=1.14–1.20), alkali-calcic ([Na₂O+K₂O]–CaO=7.68–8.57), and magnesian (FeO_t/(FeO_t+MgO)=0.76), with relatively high normative corundum contents (3.65–4.74).

Trace elements contents is also uniform for the whole set of analysed samples (Table 1). The values obtained are close to those of the total-crust composition (Rudnick and Gao, 2003) with near flat normalized patterns respect to the total-crust (Fig. 5A). These flat patterns are only modified by the relatively marked depletions in Sr and Ti, and the

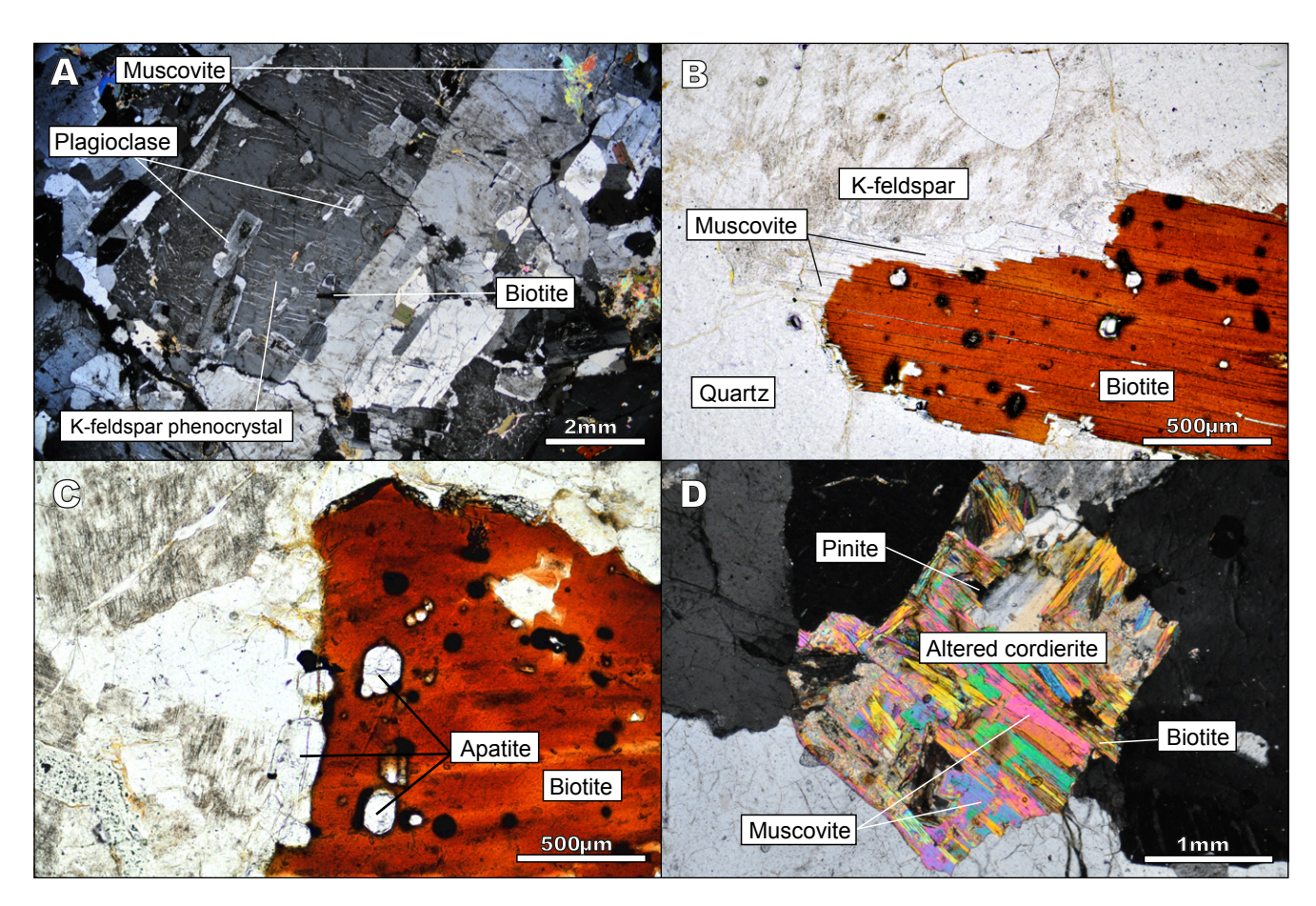


FIGURE 3. Optical microscope images of thin sections (A and D in cross-polarized light, B and C with parallel nicols). A) Oriented inclusions in perthitic K-feldspar phenocrystal. B) Detail of secondary muscovite growth on biotite edges. C) Apatite concentrate partially included in a mineral inclusion-rich biotite crystal. D) Completely altered idiomorphic cordierite.

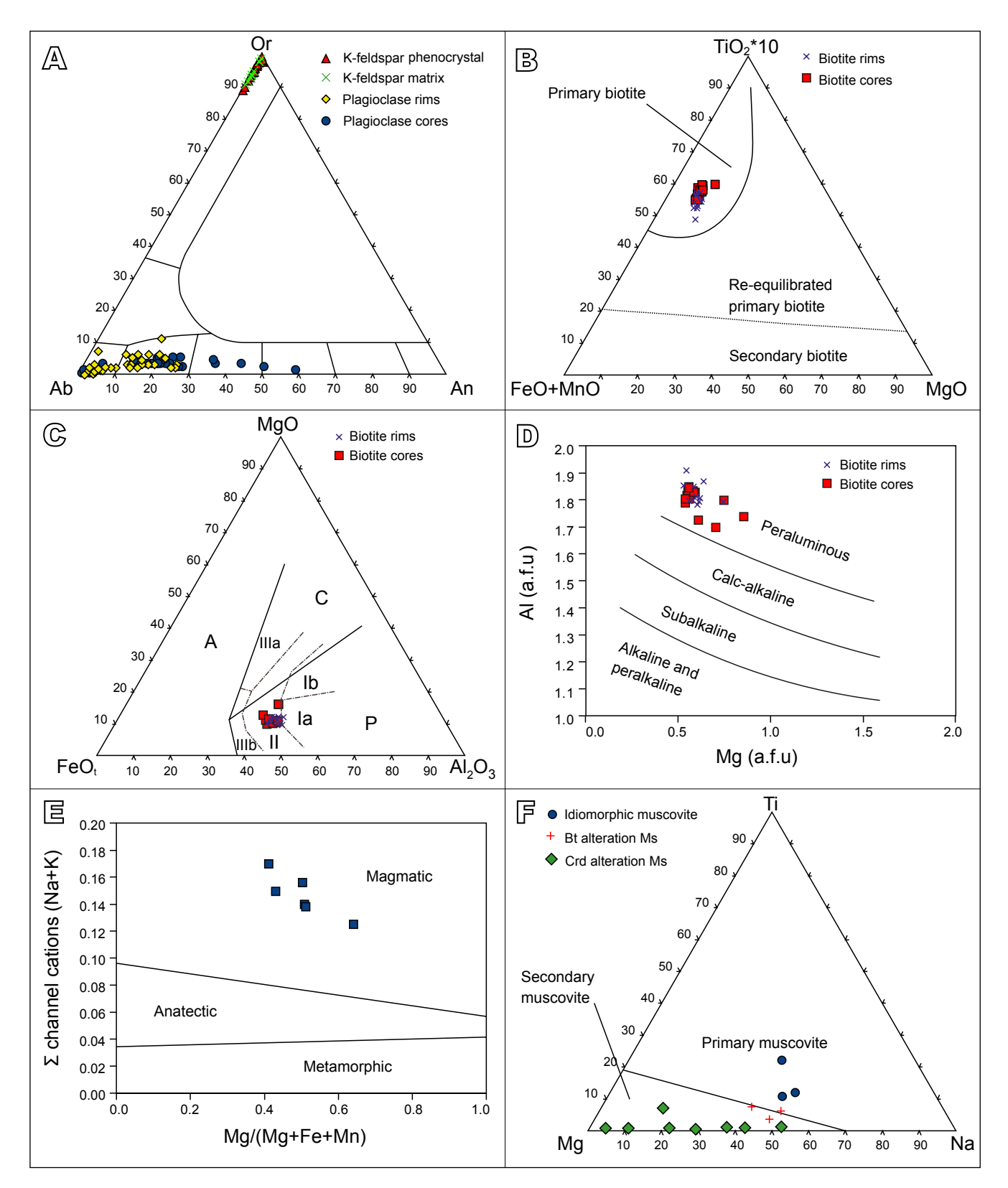


FIGURE 4. A) Ab–An–Or ternary diagram showing plagioclase and K-feldspar compositions of the Valdepeñas monzogranite. B) TiO₂–(FeO_t+MnO)–MgO ternary diagram for biotite classification (Nachit *et al.*, 2005). C) Magmatic series discrimination diagram based on biotite compositions; solid lines (Abdel-Raman, 1994) divide the A (alkali), C (calc-alkali), and P (peraluminous) fields. Dashed lines (Rossi and Chevremont, 1987) limit the following fields: la (Limousin type alumino-potassic), lb (Guéret type alumino-potassic), ll (calc-alkaline), llla (Mg-potassic monzonitic), lllb (Fe-potassic monzonitic). D) Magmatic series discrimination diagram based on the composition of biotite (Nachit *et al.*, 1985). E) Classification diagram for cordierite (Pereira and Bea, 1994). F) Mg–Ti–Na classification diagram for muscovite (Miller *et al.*, 1981).

enrichments in Rb and Cs (Fig. 5A).

Total rare earth elements (REE) range from 75.59 to 87.04ppm, with marked enrichments (60x-70x) in light REE (LREE) with respect to the chondrite average (Sun and McDonough, 1989), compared to the heavy REE (HREE; 4x-5x chondrite; Fig. 5B). Chondrite-normalized REE patterns reveal similar fractionation of LREE ([La/Sm]_N=2.5-2.6) and HREE until Ho ([Gd/Ho]_N=2.8-3.0), with a remarkable change in the patterns slope after Ho ([Ho/Lu]_N=1.2-1.3), and a Eu negative anomaly (Eu/Eu*=0.43-0.48).

ZIRCON U-Th-Pb GEOCHRONOLOGY

Backscattered electron microscopy images of zircons revealed the common occurrence of internal structures with inherited cores and rims showing different characteristics (Fig. 6). To check the possibility of different ages in those discerned areas, a total of 96 U-Pb analyses were done in 79 grains of zircon by LA-ICP-MS. The signal obtained in each analysis was carefully checked in order to discard the presence of common Pb that cannot be properly corrected by this method or of any other analytical problem. Finally, 54 analyses were considered valid for an age interpretation (Table 2). The representation of all the analysis in the Concordia diagram (Fig. 6B) shows definite differences in the results obtained pointing to at least two groups of ages within these samples.

Hence, out of the total analysis, a group of concordant values, most of them from rim or outer areas, allows to assign an emplacement age to the Valdepeñas pluton of 303±3Ma, obtained as weighing the average of ²⁰⁶Pb/²³⁸U ages of individual analyses (Fig. 6C). Another group corresponds to 24 spots located mainly at inherited cores, providing ages between 552Ma and 650Ma. Although these 24 results do not define a concordant age, a ²⁰⁶Pb/²³⁸U mean age of 599±12Ma (Fig. 6D) can, nonetheless, be obtained. Finally, a small number of analyses point to. at least, another older zircon formation event (Fig. 6A; Table 2), although it would be necessary to obtain more results in order to consider further these older values.

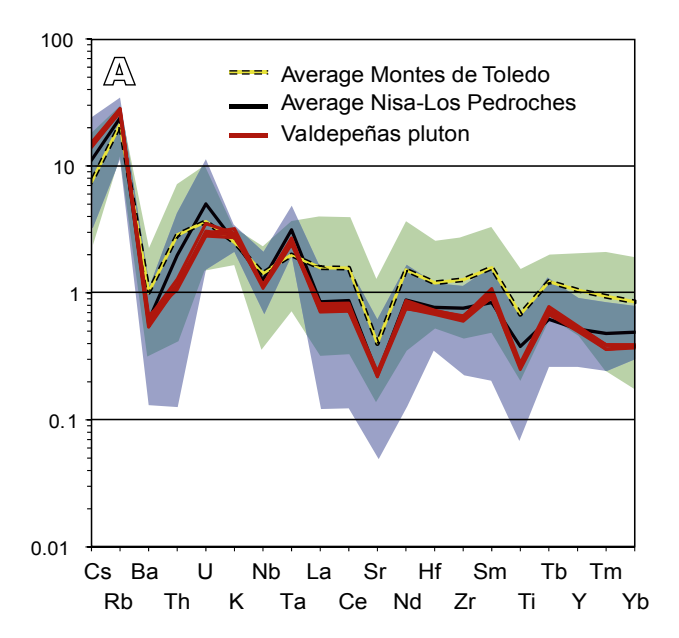
WHOLE-ROCK ISOTOPE GEOCHEMISTRY

Three monzogranitic samples were selected for whole-rock Rb-Sr and Sm-Nd isotope characterization. The relatively homogeneous Rb, Sr, Sm and Nd concentrations of the analysed rocks (Table 1) are also reflected in their ⁸⁷Rb/⁸⁶Sr, ⁸⁷Sr/⁸⁶Sr, ¹⁴³Nd/¹⁴⁴Nd, and ¹⁴⁷Sm/¹⁴⁴Nd isotopic ratios, which vary in a narrow

range (Table 3). Considering the zircon crystallization age of the Valdepeñas monzogranite (303±3Ma), initial $^{87}\mathrm{Sr/^{86}Sr}$ ratios and $\epsilon\mathrm{Nd}$ values were calculated at 300Ma. Two samples show almost identical $^{87}\mathrm{Sr/^{86}Sr}$ and $\epsilon\mathrm{Nd}$ values, and the third one shows slightly lower $^{87}\mathrm{Sr/^{86}Sr}$ ratios and less negative $\epsilon\mathrm{Nd}$ values (Table 3). Nevertheless, the three samples give very similar results (Sr_{300Ma}=0.706–0.710; Nd_{300Ma}=0.511909–0.511968), which obviously does not allow any whole-rock radiometric age estimation of the pluton.

TABLE 1. Major (in wt.%) and trace element (in µg/g) data of the Valdepeñas monzogranite

Sample	Vldp 01	Vldp 02	Vldp 03	Vldp 04	Vldp 05
SiO ₂	72.75	72.65	72.87	71.56	72.42
Al_2O_3	14.50	14.62	14.64	14.92	14.69
TiO_2	0.20	0.19	0.19	0.18	0.19
CaO	0.69	0.67	0.68	0.66	0.72
$Fe_2O_3^t$	1.38	1.54	1.46	1.65	1.44
K_2O	5.32	5.16	4.94	5.80	5.30
MgO	0.42	0.48	0.43	0.48	0.40
MnO	0.02	0.02	0.02	0.03	0.02
Na_2O	3.20	3.38	3.42	3.43	3.50
P_2O_5	0.30	0.30	0.29	0.30	0.30
LOI	1.18	0.91	0.99	0.91	0.93
Total	99.96	99.91	99.93	99.91	99.91
Ba	289	246	302	258	267
Co	103	48.3	81.8	87.8	85.5
Cr	3.59	29.4	7.64	14.8	6.44
Cs	28.0	28.6	28.9	30.4	29.4
Hf	2.71	2.66	2.61	2.51	2.68
Nb	9.06	9.12	9.27	9.16	8.71
Ni	<mdl< td=""><td>27.2</td><td>25.0</td><td>37.4</td><td>26.7</td></mdl<>	27.2	25.0	37.4	26.7
Pb	27.8	27.9	26.9	29.3	27.5
Rb	297	291	294	311	309
Sc	1.00	0.54	<mdl< td=""><td>3.00</td><td><mdl< td=""></mdl<></td></mdl<>	3.00	<mdl< td=""></mdl<>
Sn	16.91	14.15	16.12	14.41	15.85
Sr	69.37	73.33	71.45	72.39	75.41
Ta	1.77	1.82	1.77	1.89	1.69
Th	7.17	6.40	5.94	6.20	6.55
U	4.58	3.98	3.65	3.83	3.77
V	12.75	12.55	13.08	13.58	12.29
Y	10.36	9.9	9.79	9.58	10.29
Zn	58.74	60.29	60.79	65.49	61.07
Zr	85.86	83.17	83.67	78.58	87.02
La	16.34	14.75	14.29	14.43	15.54
Ce	35.82	32.61	31.14	31.53	33.99
Pr	4.72	4.19	4.04	4.10	4.43
Nd	17.46	15.55	14.91	15.14	16.38
Sm	4.21	3.75	3.59	3.63	3.93
Eu	0.52	0.51	0.50	0.51	0.53
Gd	3.29	2.96	2.85	2.85	3.09
Tb	0.47	0.43	0.41	0.41	0.44
Dy	2.19	2.04	1.96	1.98	2.12
Но	0.30	0.29	0.28	0.28	0.30
Er	0.75	0.72	0.70	0.69	0.75
Tm	0.11	0.11	0.11	0.10	0.11
Yb	0.75	0.73	0.72	0.71	0.75
Lu	0.11	0.10	0.10	0.10	0.11



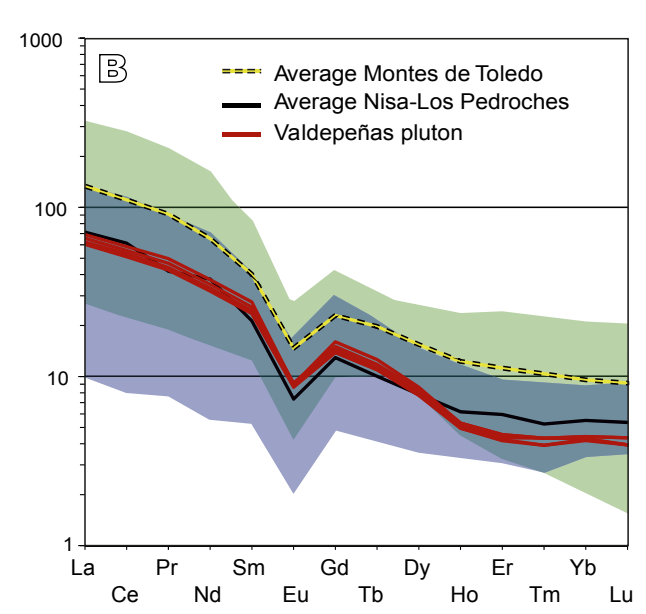


FIGURE 5. A) Total-crust-normalized trace element diagrams of the Valdepeñas monzogranite. Normalization values taken from Rudnick and Gao (2003). B) REE chondrite-normalized diagram of the Valdepeñas monzogranite. Normalization values from Sun and McDonough (1989). In both diagrams, the green field corresponds to the Montes de Toledo batholith (Merino Martínez *et al.*, 2014) and the blue field to the Nisa Alburquerque-Los Pedroches alignment (Alonso Olazabal, 2001; González-Menéndez, 2002).

DISCUSSION

Magma sources of the Valdepeñas pluton

Mineral and whole-rock composition of the studied samples of the Valdepeñas pluton allow to classify them as S-type, cordierite-bearing peraluminous monzogranites. They could have been derived directly from the melting of crustal sources (metasedimentary or metaigneous), although they could also have been generated by mixing/assimilation of crustal rocks with/by mantle-derived melts, or they could have even been generated by the extreme differentiation of mantle-derived melts (*e.g.* Villaseca *et al.*, 1998b; Bea *et al.*, 1999; Castro *et al.*, 1999; Bea *et al.*, 2003). Crustal mafic metaigneous sources will be excluded of the present discussion because they usually produce K-poor melts of tonalitic or trondhjemitic compositions (*e.g.* Sylvester, 1998).

CaO/Na₂O ratios in Valdepeñas (0.19-0.21) are lower than 0.3, discarding the involvement of significant volumes of mafic melts during a hypothetical magma mixing process (Sylvester, 1998), pointing rather to a metapelitic source. Nevertheless, Eu/Eu* values (Eu/Eu*= 0.43-0.48) indicate that plagioclase fractionation is playing a role, and the CaO/Na2O ratio may be altered from the ones representing pure granite melts, which impedes to discard a metaigneous source. Moreover, the low CaO content in Valdepeñas (0.66-0.72 wt.%) is far from that of experimental melts obtained by melting-assimilation tests with mafic metaigneous and metamorphic protoliths (e.g. CaO=1.48-3.23 wt.%; Patiño Douce, 1995). In the A-B diagram of Debon and Le Fort (1983; modified by Villaseca et al., 1998a), the samples of Valdepeñas are projected in the peraluminous category, concretely in the felsic peraluminous field but near to the moderately peraluminous field, showing relatively low values (slightly <50) of both A and B parameters (Fig. 7), which points to a crustal origin. According to Villaseca et al. (1998a), the apparent absence of MME (numerous in moderately peraluminous granitoids) is consistent with their projection in the felsic peraluminous field (Fig. 7). Nevertheless, their low modal proportions of muscovite and the presence of biotite and cordierite as mafic minerals do not fit completely the expected characteristics of the granitoids of this field. Compared to experimental melts obtained from crustal sources (Patiño Douce and Johnston, 1991; Montel and Vielzeuf, 1997), the composition of studied samples overlap that of melts derived from pelite and greywacke sources (Fig. 7). Furthermore, they do not match the composition of the most evolved terms of cafemic and alumino-cafemic magmatic series, which derive from mantle and hybrid (mantle-crust) sources (Debon and Le Fort, 1983). Whole-rock major element geochemistry data would indicate, in a first approach, an exclusively crustal source for the Valdepeñas magmas.

The obtained weighted average of ²⁰⁶Pb/²³⁸U age for the Valdepeñas pluton allows to assign an emplacement age of 303±3Ma, and let us classify it as a late- to post-D3 granitoid (*e.g.* Dias *et al.*, 1998). The radiometric age is in the range of ages of peraluminous intrusions of the Montes de Toledo batholith (297–316Ma; Merino Martínez *et al.*, 2014) and the Central Extremadura batholith (296–309Ma;

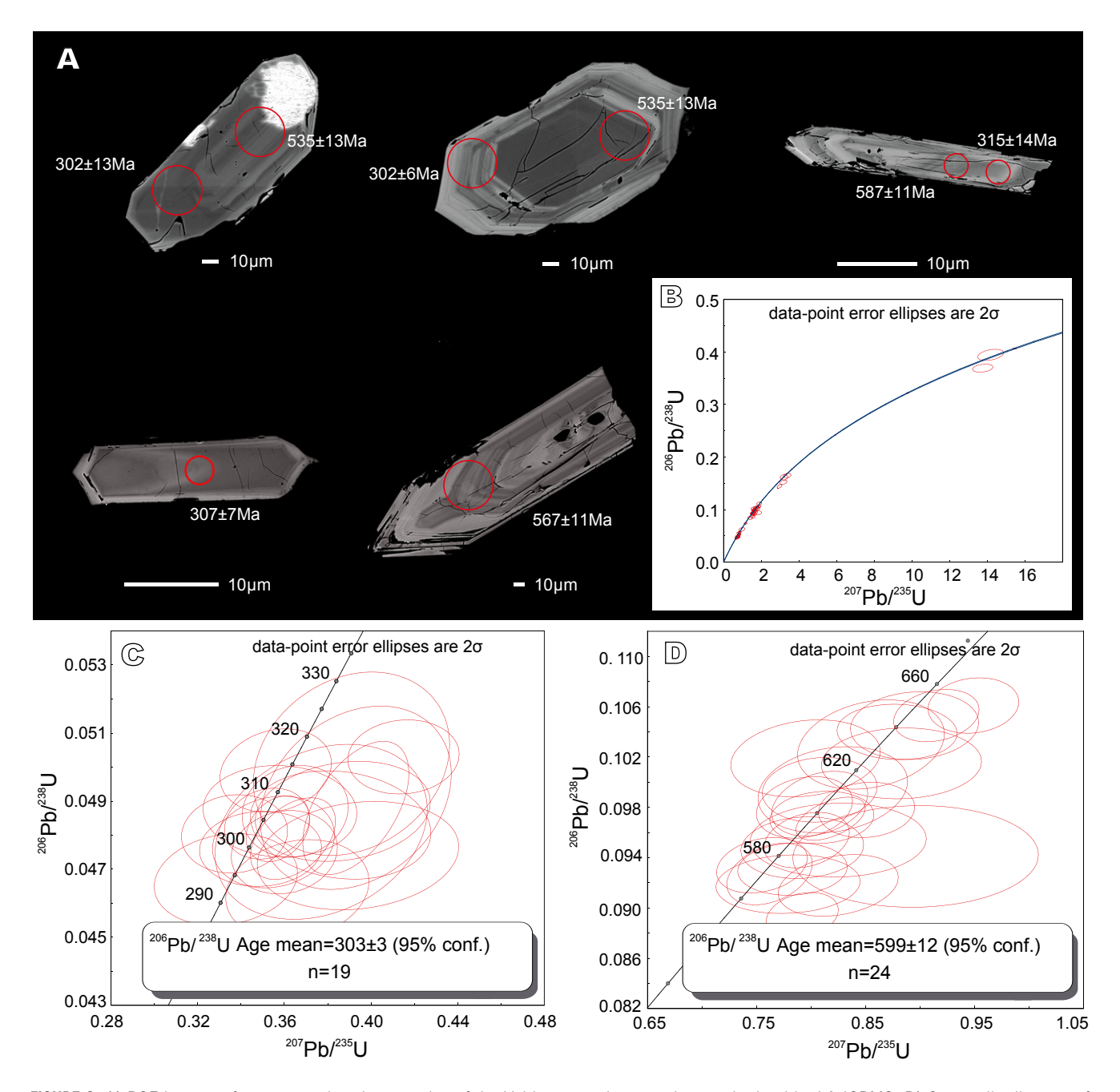


FIGURE 6. A) BSE images of representative zircon grains of the Valdepeñas pluton and ages obtained by LA-ICPMS. B) Concordia diagram of 54 analyses obtained by LA-ICPMS. C) and D) represent U-Pb Concordia diagrams and weighted average ²⁰⁶Pb/²³⁸U ages of rims/outer areas (C) and inherited cores (D) analyses, respectively.

Carracedo *et al.*, 2005; Gutiérrez-Alonso *et al.*, 2011), and it would be slightly younger than those obtained for the Nisa-Alburquerque-Los Pedroches alignment (304–314Ma; García de Madinabeitia *et al.*, 2003; Carracedo *et al.*, 2005, 2009; Solá *et al.*, 2009; Gutiérrez-Alonso *et al.*, 2011).

Trace element patterns normalized to total-crust (Rudnick and Gao, 2003) of the Valdepeñas monzogranite are similar to the average normalized pattern of the Nisa-

Alburquerque-Los Pedroches alignment granites, while markedly depleted (in the most compatible elements) when compared to that of the Montes de Toledo alignment (Fig. 5A). Similarly occurs with the chondrite-normalized REE patterns, which are practically equal to the average of the Nisa-Alburquerque-Los Pedroches alignment granites (slightly depleted after Ho), and markedly depleted regarding the average of the Montes de Toledo alignment (Fig. 5B). A comparison to other rocks of the Cáceres-Valdepeñas alignment has not been attempted

 TABLE 2. U-Th-Pb zircon LA-ICPMS analyses. For a, b, c key see the figure caption of Table 3

Spot _				Data for Wetherill plot				Ages					
name	U	Th	Pb	²⁰⁷ Pb/ ²³⁵ U	2s ^b	$^{206}Pb/^{238}U$	$2s^{b}$	Rho	²⁰⁶ Pb/ ²³⁸ U	2s (abs)b	207 Pb/ 235 U	2s (abs)b	% cond
1	206	427	2	0.88	5%	0.104	2%	-0.05	638	10	634	25	10
4	313	638	1	0.81	5%	0.097	2%	0.10	598	10	593	22	10
7	271	273	2	0.36	6%	0.045	2%	0.09	285	6	309	17	92
9	84	92	4	0.39	9%	0.048	3%	-0.15	304	8	321	25	9:
10	100	113	3	0.36	8%	0.049		-0.05	307	7	301	21	10
1	163	175	3	0.39	9%	0.049		0.18	307	7	322	23	9
4	155	148	5	0.42	7%	0.053		0.09	335	10	348	22	9
15	164	276	53	0.36	4%	0.033		0.43	302	6	314	12	9
	99												
16		193	3	0.78	5%	0.093		0.08	574	10	576	23	10
17	82	135	7	0.48	13%	0.062		0.33	389	18	392	43	9
18	171	223	29	0.36	3%	0.048		0.29	303	5	309	9	9
9	860	1954	1	0.90	5%	0.105		0.09	640	13	647	27	9
20	372	1165	3	1.49	4%	0.144	2%	0.54	868	16	921	21	9
22	999	963	4	0.43	5%	0.052	2%	0.40	326	7	360	15	9
23	680	616	3	0.42	5%	0.050	2%	0.07	316	5	350	15	9
24	61	125	2	0.90	10%	0.094	4%	0.03	579	19	615	52	9
25	198	375	1	0.78	7%	0.092	2%	0.10	567	11	568	31	10
26	139	455	2	1.60	5%	0.162		0.09	964	22	959	32	10
27	121	414	2	1.69	5%	0.165		0.22	983	20	995	29	9
28	111	216	1	0.83	8%	0.095		0.04	587	14	584	38	10
29	132	271	1	0.88	7%	0.102		0.05	623	13	629	34	9
33	332	336	3	0.36	6%	0.102		0.03	299	6	309	15	9
						0.048			304				
35	101	117	12	0.35	5%			0.17		5	303	12	10
37	540	1041	2	0.85	4%	0.098		0.10	601	11	621	20	9
38	969	1942	3	0.82	3%	0.097		0.51	598	8	605	14	9
12	161	257	2	0.58	5%	0.074		0.19	459	8	463	20	9
14	1115	2147	2	0.79	3%	0.089	2%	0.25	552	9	594	15	9
15	112	307	40	0.39	5%	0.049	3%	0.52	307	10	335	15	9
18	129	137	4	0.35	7%	0.048	2%	0.05	300	6	298	17	10
2_09	103	188	3	0.71	7%	0.084	3%	-0.04	521	15	536	30	9
P 10	62	85	34	0.39	9%	0.050	4%	0.21	315	14	333	27	9
P 11	888	1628	1	0.80	4%	0.095	2%	0.27	587	11	591	18	9
P 13	71	100	25	0.40	10%	0.056		0.27	350	11	341	30	10
P 14	255	252	4	0.40	8%	0.053		0.29	330	8	335	22	9
P 15	189	324	3	0.76	5%	0.093		0.26	575	11	564	19	10
P 16	310	559	2	0.70	7%	0.093		0.20	610	16	597	32	10
_													
P_17	300	529	2	0.79	5%	0.098		0.21	602	12	584	20	10
P_18	336	622	2	0.86	6%	0.103		0.24	632	17	629	30	10
P_19	117	116	6	0.43	7%	0.057		0.23	356	9	359	21	9
20	705	1179	1	0.79	6%	0.095		0.09	584	12	586	26	10
P_21	176	189	3	0.37	5%	0.049		0.10	306	7	313	15	9
22	131	142	4	0.36	6%	0.048	2%	0.15	301	7	303	17	9
2_24	79	91	3	0.39	10%	0.047	3%	0.16	299	8	325	27	9
25	149	1085	2	6.88	3%	0.369	2%	0.27	2025	29	2089	28	9
26	128	308	7	0.95	4%	0.106	2%	0.13	650	10	673	18	9
27	124	290	7	0.92	3%	0.105		0.23	645	10	655	18	9
28	175	371	2	0.80	7%	0.102		0.18	625	15	582	31	10
29	156	344	3	0.95	6%	0.112		0.20	682	14	665	29	10
230	171	174	5	0.34	6%	0.048		0.20	302	6	293	16	10
	205	211							293				
21			2	0.37	7%	0.046		0.17		7	318	22	9
2.34	514	1497	2	1.59	5%	0.152		0.40	912	19	958	31	9
235	558	958	2	0.78	6%	0.087		0.25	535	13	582	30	9
2_36	51	69	16	0.38	11%	0.048		0.26	302	13	320	29	9
_37	50	67	20	0.39	9%	0.049		0.26	309	13	333	26	9
2_38	90	93	3	0.33	8%	0.047		0.16	294	7	282	21	10
2_39	283	268	2	0.33	7%	0.045	2%	0.08	281	6	285	17	9
- P_40	387	731	2	0.83	5%	0.092		0.26	566	12	604	25	9
2_43	88	639	4	7.09	4%	0.395		0.37	2142	41	2120	34	10
2 44	175	180	6	0.36	6%	0.050		0.17	314	6	306	16	10
2_46	1415	2978	1	0.36	4%	0.030		0.17	571	12	569	18	10
P_47	507	1042	2	0.81	5%	0.099		0.10	611	12	595	24	10
P_48	455	916	1	0.81	4%	0.098	2%	0.31	604	12	599	20	10

TABLE 3. Sr and Nd isotope compositions of the Valdepeñas monzogranite

Sample	Rb ^a	Sr ^a	87 Rb/ 86 Sr	$^{87}\mathrm{Sr}/^{86}\mathrm{Sr}$ b	⁸⁷ Sr/ ⁸⁶ Sr _{300Ma}	
Vldp 01	297	69.4	12.4	0.764361 (16)	0.711253	
Vldp 02	291	73.3	11.5	0.756689 (16)	0.707424	
Vldp 03	294	71.5	12.0	0.761611 (16)	0.710544	
Sample	Sm ^a	Nd ^a	¹⁴⁷ Sm/ ¹⁴⁴ Nd	¹⁴³ Nd/ ¹⁴⁴ Nd ^{b,c}	¹⁴³ Nd/ ¹⁴⁴ Nd _{300Ma}	(εNd) _{300Ma}
Vldp 01	3.57	14.7	0.1471	0.512222 (7)	0.511933	-6.26
Vldp 02	3.36	14.2	0.1428	0.512251 (7)	0.511971	-5.53
Vldp 03	3.24	13.3	0.1470	0.512200 (5)	0.511911	-6.68

a: Concentrations are in µg/g.

because of the difficulty to obtain enough trace element data from literature. We have only considered the case of the Logrosán cupola, which shows similar normalized REE patterns to those of the Valdepeñas monzogranite (Chicharro *et al.*, 2014).

Valdepeñas monzogranite shows high $^{86}Sr/^{87}Sr_{300Ma}$ ratios (0.707424–0.711253) and ϵNd_{300Ma} values between -5.53 and -6.68 (Table 3). In the $^{86}Sr/^{87}Sr_{300Ma}\!\!-\!\epsilon Nd_{300Ma}$ diagram (Fig. 8), studied samples plot in the field of the felsic granulites derived from the lower crust of the Spanish Central System (SCS; Villaseca et al., 1998b 1999) and the anatexites of the Anatectic Complexes of the Ávila Batholith (ACAB; Bea et al., 1999, 2003), but out of the field of the metasediments of the Schist and Greywacke Complex (Fig. 8). Although the ENd_{300Ma} values diverge slightly upwards from the "crustal source trend" of Castro et al. (1999; Fig. 8), these values and elevated initial 86Sr/87Sr ratios suggest a crustal provenance of the magmas that generated the studied monzogranite, in agreement with their marked peraluminous character (e.g. McCulloch and Chappell, 1982; Fitton et al., 1988; Saunders et al., 1988). Moreover, the isotopic signature of Valdepeñas monzogranite allows to discriminate between metapelitic and felsic metaigneous sources in favour of the latter. In the Montes de Toledo batholith, similar ⁸⁶Sr/⁸⁷Sr_{300Ma} ratios and εNd_{300Ma} values of Type-3 granodiorites and monzogranites are related with Ordovician felsic peraluminous metaigneous sources (Merino Martínez et al., 2014). Similarly, the 86Sr/87Sr_{300Ma} ratios of Valdepeñas monzogranite are comparable to those of the Nisa-Alburquerque batholith granitoids (González Menéndez, 1998) and the Campanario-La Haba pluton (Alonso Olazabal, 2001), though ENd_{300Ma} values differ slightly in both cases. In the Nisa-Alburquerque batholith, it is suggested a metaigneous source only for the Central Facies B, while in the Campanario-La Haba

pluton is suggested a metapelitic source with variable mantle contribution (González Menéndez, 1998; Alonso Olazabal, 2001). In the Central Extremadura batholith of the Cáceres-Valdepeñas alignment, the "Serie Mixta" granitoids show similar Sr-Nd isotopic signatures to those mentioned of the Nisa-Alburquerque-Los Pedroches alignment, whereas Plasenzuela and Montánchez granites show noticeably higher 86Sr/87Sr_{300Ma} ratios and less negative eNd_{300Ma} values (Castro et al., 1999). Finally, the Logrosán cupola shows slightly higher 86Sr/87Sr_{300Ma} ratios and higher εNd_{300Ma} values (Chicharro et al., 2014) than those of the Valdepeñas monzogranite. The "Serie Mixta" granitoids source is still a matter of controversy, but mantle contribution is suggested (Castro et al., 1999; García-Moreno, 2004). On the contrary, the granitoids of the Logrosán cupola are related to the partial melting of heterogeneous Neoproterozoic metasediments (Chicharro et al., 2014).

The 552-650Ma Cryogenian to Ediacaran ages of inherited zircon cores in Valdepeñas monzogranite fit with the abundant inheritance of zircons of Neoproterozoic (mostly Ediacaran), Cambrian and Ordovician ages found in some CIZ granitoids (Fernández-Suárez et al., 2011; Orejana et al., 2012; Villaseca et al., 2012; Merino Martínez et al., 2014). Moreover, similar inherited ages have also been determined in zircons of lower crustal granulite xenoliths of the SCS (Fernández-Suárez et al., 2006), in the Cambrian-Ordovician metavolcanics and Lower Paleozoic metagranitic orthogneisses of central and NW Iberia (Montero et al., 2007; 2009; Talavera et al., 2008, 2013; Villaseca et al., 2016), and as discrete grains in metasedimentary rocks of the Schist and Greywacke Complex (Talavera et al., 2012). As mentioned above, major element composition and Sr-Nd isotopic signature of the Valdepeñas monzogranite are consistent with metaigneous crustal sources. The presence of inherited zircon cores of

b: The 87Sr/86Sr ratio of the NBS 987 standard measured during the period of the analyses was 0.710269. 2SD=0.000006 (n=2).

Errors are expressed as 2SE from internal measurements and refer to the least significant digit.

c: During the period of measurements. The La Jolla isotopic standard gave a value of 143Nd/144Nd=0.511860. 2SD=0.000008 (n=1).

Errors are expressed as 2SE from internal measurements and refer to the least significant digit.

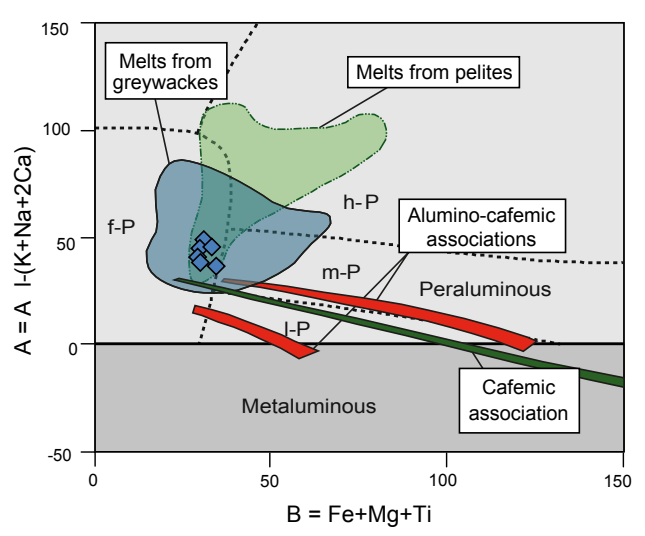


FIGURE 7. A-B diagram of Debon and Le Fort (1983; modified by Villaseca *et al.*, 1998a) including the fields of experimental melts derived from pelitic (Patiño Douce and Johnston, 1991) and greywacke sources (Montel and Vielzeuf, 1997). Blue diamonds correspond to the Valdepeñas pluton samples.

552–650Ma suggests that the protolith for the generation of the Valdepeñas monzogranitic magma might have most likely been of Ediacaran age. This means that the protolith would be similar to the one of the metavolcanics and Lower Paleozoic metagranitic orthogneisses of the SCS (*e.g.* Bea *et al.*, 1999, 2003; Villaseca *et al.*, 2016).

The emplacement age obtained for the Valdepeñas pluton (303±3Ma; Gzhelian) coincides with that of the gravitational collapse and erosive dismantling of the Variscan orogeny (Martínez Catalán et al., 2009). This late extensional regime could have led to an important decompression of the upper mantle and the lower thickened crust. Decompression could have induced mantle melting and emplacement of mafic magmas in the middle crust. The heat provided by these mafic magmas could have contributed to the increase of the already high temperatures (thermally incubated during crustal thickening) of the materials forming lower and middle portions of the crust, and their melting generated peraluminous magmas (Annen et al., 2006; Castro, 2014). Nevertheless, in the CIZ, basic rocks related to peraluminous granitoids are scarce, or notably younger than crustal melting events (Villaseca et al., 1998b, Bea et al., 1999; Bea et al., 2006; Merino Martínez et al., 2014). In this crustal thickening scenario mantle contribution would imply a normal conductive heat through the base of the lithosphere (Patiño Douce et al., 1990). In this context, the main heat supply for crustal melting would be the radiogenic heating due to the enrichment of the crustal sources in heatproducing elements, such as K, Th and U (Bea, 2012). According to this author, a fertile continental crust (more radioactive than the average continental crust)

can generate large granitic magmatism after 30–40Ma of thermal maturation. Thus, radiogenic heating of a crustal metaigneous source could induce the generation of the magmas that fed the Valdepeñas pluton. The extrapolation of this petrogenetic model to the origin of peraluminous granitoids in the southern CIZ must be taken with caution since whole-rock geochemistry of the peraluminous granitoids is variable in detail, and whole-rock isotope characterization data are still scarce.

Geothermometry from whole-rock composition

Accessory minerals play a decisive role in petrogenetic studies of granitoids since they directly control the response of isotopic systems and dictate the geochemical variation of different elements, especially that of trace elements. In the case of peraluminous granitoids, zircon, apatite and monazite are key minerals in this case (Bea, 1996a, 1996b; Janoušek *et al.*, 2016 and references therein).

Harrison and Watson (1984) defined an expression for apatite saturation behaviour in melts with 0–10% of H₂O and temperatures of 850°C to 1500°C but, because of the higher potential of peraluminous melts, Bea *et al.* (1992) and Pichavant *et al.* (1992) proposed improvements for this equation. Nevertheless, for rocks with SiO₂>70 wt.% these equations are very sensitive to small variations in whole-rock P₂O₅ concentrations, and small analytical errors could derive in significant changes in calculated saturation temperatures (Janoušek, 2006). Using the GCDkit software (Janoušek, 2006;

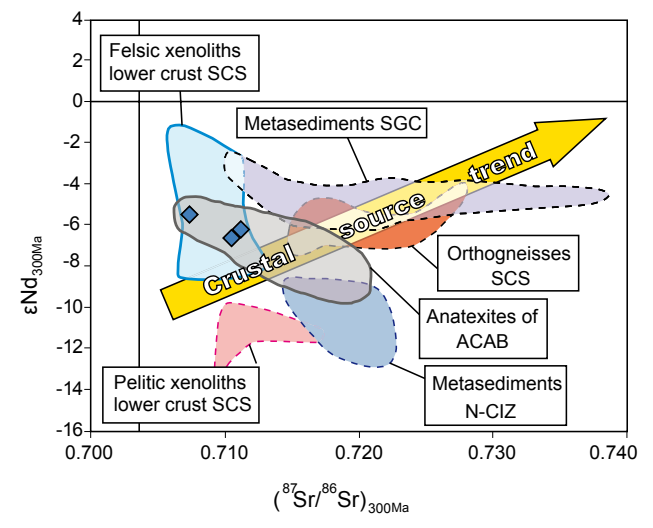


FIGURE 8. £Nd_{300Ma}-Sr_{i300Ma} diagram based on Villaseca *et al.* (2008). The crustal source trend is taken from Castro *et al.* (1999). Blue diamonds correspond to the Valdepeñas pluton samples. SCS: Spanish Central System; SGC: Schist and Greywacke Complex; N-CIZ: Northern Central Iberian Zone; ACAB: Anatectic Complexes of the Ávila Batholith.

TABLE 4. Apatite, zircon and monazite saturation temperatures of the Valdepeñas pluton

Sample	Vldp 01	Vldp 02	Vldp 03	Vldp 04	Vldp 05
n	-	-	-	6	6
$P_2O_5\%$ in apatite (\bar{x})	-	-	-	42.74	42.57
SiO ₂ % whole-rock	72.75	72.65	72.87	71.56	72.42
P ₂ O ₅ % whole-rock	0.30	0.30	0.29	0.30	0.30
A/CNK	1.18	1.18	1.20	1.14	1.15
T°C Apatite microprobe (Pichavant et al., 1992)	-	-	-	673	667
T°C Apatite (Pichavant et al., 1992)	639	633	622	673	667
T°C Zircon (Watson and Harrison, 1983)	746	743	745	734	744
T°C Monazite (Montel, 1993)	762	753	753	742	751

Janoušek *et al.*, 2006), which assumes a 42 wt.% of P_2O_5 in apatite, saturation temperatures for apatite in the Valdepeñas monzogranite were calculated. The temperatures provided by the methods of Harrison and Watson (1984) and Bea *et al.* (1992) seem to be overestimated (~900–1050°C), while those estimated with the expression of Pichavant *et al.* (1992) are more suitable for these rocks, comprising temperatures of 622–673°C (Table 4). An identical temperature range of 667–673°C is obtained for the analysed two samples using that expression and apatite electron microprobe data (Table 4).

Given their significance for geochronology and the fact that they register high temperature crustal processes, the solubility of zircon and monazite in felsic melts has attracted special interest in the last decades (Hanchar and Watson, 2003 and references therein; Janoušek, 2006). Watson and Harrison (1983) carried out an experimental work and proposed an expression for the solubility of zircon in calc-alkaline melts as a function of the temperature. In the Valdepeñas pluton, most zircons have inherited cores, which suggests a source saturated in Zr. In this case, the equation of Watson and Harrison (1983) could overestimate the saturation temperature of zircon (Miller et al., 2003; Harrison et al., 2007). This equation has been refined by Bohenke et al. (2013) and concluded that, except those cases in which the M ($[Na + K + 2Ca]/[Al \times Si]$) and Zr values are high, the new model predicts similar temperatures for most melt compositions and temperatures to that of Watson and Harrison (1983). Considering the M values (1.22–1.32) and Zr concentrations (78.58–87.02ppm) of the Valdepeñas monzogranite, even assuming that zircon saturation temperatures were overestimated, we have calculated the temperature range. Using the GCDkit software, which assumes an amount of 497,644ppm of zirconium in zircon, and using the

expression of Watson and Harrison (1983), the obtained temperature range is 734–746°C (Table 4).

Monazite is the main LREE carrier (as it can also incorporate Th and U) in Ca-poor felsic melts, which became saturated in monazite and xenotime with low amounts of REE (Bea, 1996b). From the experimental works of Rapp and Watson (1986), Montel (1993) defined an expression for monazite solubility in this type of melts. This expression, using the GCDkit software for monazite saturation temperatures in the Valdepeñas monzogranite gives a range of $742-762^{\circ}$ C (Table 4). Considering the whole-rock P_2O_3 determination problem mentioned above and the presence of inherited zircon cores, the most suitable temperature range of crystallization of the Valdepeñas monzogranite are those obtained from monazite ($742-762^{\circ}$ C; Table 4).

Using the solubility of accessory minerals above mentioned, González-Menéndez (1998) and Alonso Olazabal (2001) determined the emplacement temperatures of the Nisa-Alburquerque batholith and the Campanario-La Haba pluton, respectively, obtaining a range of 640–800°C. Similarly, Merino Martínez et al. (2014) determined the emplacement temperatures of the Montes de Toledo batholith, obtaining values of 630-880°C, thus very close to those of Nisa-Alburquerque-Los Pedroches aligment. On the basis of experimental studies with samples of the Cabeza de Araya pluton, García-Moreno et al. (2007) poproposed temperatures of 700-850°C for the peraluminous magmas of the Cáceres-Valdepeñas alignment. These values are similar to those obtained for the aforementioned two alignments and to those obtained in our study. The emplacement temperature range (742-762°C), for the melts that generated the Valdepeñas pluton, would be, therefore, within the range of the reported temperatures for peraluminous intrusive rocks elsewhere in the CIZ.

CONCLUSIONS

The Valdepeñas pluton is the easternmost outcrop of the Cáceres-Valdepeñas magmatic alignment (southern Central Iberian Zone) and is constituted by a cordieritebearing porphyritic peraluminous monzogranite. The whole-rock geochemistry of this monzogranite is closer to the granitoids of the Nisa-Alburquerque-Los Pedroches magmatic alignment rather than to the one of the Montes de Toledo batholith. The obtained U-Pb zircon age (303±3Ma) is in accordance with most of the granitic peraluminous intrusions of the southern CIZ. $^{86}Sr/^{87}Sr_{300Ma}$ ratios (0.707424–0.711253) and εNd_{300Ma} values (-5.53 to -6.68), coupled with wholerock geochemical data, suggest a crustal metaigneous source of the parental magma of the Valdepeñas monzogranite. This hypothesis is also supported by the U-Pb ages (552-650Ma) of inherited zircon cores found in this monzogranite, which point to Cambrian-Ordovician metavolcanics and/or Lower Paleozoic metagranitic orthogneisses of central Iberia as the most likely sources. The melting of these sources at a latecollisional Variscan stage could be closely related to heat-producing radiogenic elements (K, Th, and U) of the crust. The estimated emplacement temperature of the Valdepeñas monzogranite is 742–762°C.

ACKNOWLEDGMENTS

Financial support by the Spanish Ministerio de Ciencia e Innovación (grant CGL2015-63530-P) and the University of the Basque Country UPV/EHU (Grupo Consolidado project GIU15/05) is acknowledged. J. Errandonea-Martin would also like to thank the grant from the UPV/EHU 2014 program for the formation of research scientists. F. de la Cruz at the UPV/EHU, for the help in the preparation of thin sections, as well as the technical and human support provided at the Geochronology and Isotope Geochemistry-SGIker facility (UPV/EHU, MINECO, GV/EJ, ERDF and ESF), is gratefully acknowledged. Constructive criticism by F. Bea and an anonymous reviewer are also appreciated.

REFERENCES

- Ábalos, B., Gil Ibarguchi, J.I., Sánchez Lorda, M.E., Paquette, J.L., 2012. Detrital zircon U-Pb study of early Cambrian conglomerates from the Sierra de la Demanda (N Spain): implications for West-African/Amazonian Proterozoic correlations of Iberia. Tectonics, 31, TC3003, https://doi.org/10.1029/2011TC003041.
- Abdel-Rahman, A.F.M., 1994. Nature of biotites from alkaline, calc-alkaline, and peraluminous magmas. Journal of Petrology, 35(2), 525–541. https://doi.org/10.1093/petrology/35.2.525.

- Alonso Olazabal, A., 2001. El plutón de Campanario-La Haba: caracterización petrológica y fábrica magnética. PhD Thesis, University of the Basque Country, Spain, 323pp.
- Andonaegui, P., 1990. Geoquímica y geocronología de los granitoides del Sur de Toledo. PhD Thesis. Complutense University of Madrid, Spain, 365pp.
- Annen, C., Blundy, J.D., Sparks, R.S.J., 2006. The Genesis of Intermediate and Silicic Magmas in Deep Crustal Hot Zones. Journal of Petrology, 47(3), 505–539. https://doi.org/10.1093/ petrology/egi084.
- Aparicio, A., Barrera, J.L., Casquet, C., Peinado, M., Tinao, J.M., 1977. Caracterización Geoquímica del plutonismo post-metamórfico del SO del Macizo Hespérico. Studia Geologica, XII, 9–39.
- Barbero, L., Villaseca, C., 2004. El macizo de Toledo. In: Vera, J.A. (ed.). Geología de España. Sociedad Geológica de España e Instituto Geológico y Minero de España, Madrid, 110–115.
- Barbero, L., Villaseca, C., Andonaegui, P., 1990. On the origin of the gabbro-tonalite-monzogranite association from Toledo area (Hercynian Iberian belt). Schweizerische Mineralogische Und Petrographische Mitteilungen, 70, 209–221.
- Bea, F., 1996a. Controls on the trace element composition of crustal melts. Transaction of the Royal Society of Edinburg: Earth Sciences, 87(1–2), 33–41. https://doi.org/10.1017/ S0263593300006453.
- Bea, F., 1996b. Residence of REE, Y, Th and U in Granites and Crustal Protoliths; Implications for the Chemistry of Crustal Melts. Journal of Petrology, 37(3), 521–552. https://doi. org/10.1093/petrology/37.3.521.
- Bea, F., 2012. The sources of energy for crustal melting and the geochemistry of heat-producing elements. Lithos, 153, 278–291. https://doi.org/10.1016/j.lithos.2012.01.017.
- Bea, F., Fershtater, G., Corretgé, L.G., 1992. The geochemistry of phosphorus in granite rocks and the effect of aluminium. Lithos, 29(1–2), 43–56. http://dx.doi.org/10.1016/0024-4937(92)90033-U.
- Bea, F., Pereira, M.D., Corretgé, L.G., Fershtater, G.B., 1994. Differentiation of strongly peraluminous, perphoshorous granites. The Pedrobernardo pluton, central Spain. Geochimica et Cosmochimica Acta, 58, 2609–2628. http://dx.doi. org/10.1016/0016-7037(94)90132-5.
- Bea, F., Montero, P., Molina, J.F., 1999. Mafic precursors, peraluminous granitoids, and late lamprophyres in the Avila batholith: A model for the generation of Variscan batholiths in Iberia. The Journal of Geology, 107(4), 399–419. http://dx.doi. org/10.1086/314356.
- Bea, F., Montero, P., Zinger, T., 2003. The Nature, Origin, and Thermal Influence of the Granite Source Layer of Central Iberia. The Journal of Geology, 111, 579–595. http://dx.doi. org/10.1086/376767.
- Bea, F., Montero, P., González-Lodeiro, F., Talavera, C., Molina, J.F., Scarrow, J.H., Whitehouse, M.J., Zinger, T.F., 2006. Zircon thermometry and U-Pb ion-microprobe dating of the gabbros and associated migmatites of the Variscan Toledo Anatectic Complex, Central Iberia. Journal of the Geological Society, London, 163, 847–855. DOI:10.1144/0016-76492005-143.

- Bergamín, J.F., De Vicente, G., 1985. Estructura en profundidad del granito de Pozo de la Serna (Ciudad Real), basada en determinaciones gravimétricas. Estudios Geológicos, 41, 5–6.
- Capdevila, R., Corretgé, L.G., Floor, P., 1973. Les granitoides varisques de la Meseta Ibérica. Bulletin de la Société Géologique de France, 15/7(3-4), 209-228.
- Caride de Liñán, C., 1994. Mapa Geológico de la Península Ibérica, Baleares y Canarias a escala 1:1.000.000, 1^a edición. Available at: http://info.igme.es/cartografiadigital/geologica/Geologicos1MMapa.aspx?Id=Geologico1000_(1994)&language=es. [last access: 17/11/2017]
- Carracedo, M., Gil Ibarguchi, J.I., García de Madinabeitia, S., Berrocal, T., 2005. Geocronología de los granitoides Hercínicos de la Serie Mixta: Edad U-Th-Pb_{total} de monacitas del plutón de Cabeza de Araya (Zona Centro Ibérica) y de las manifestaciones filonianas asociadas. Revista de la Sociedad Geológica de España, 18(1–2), 75–86.
- Carracedo, M., Paquette, J.L., Alonso Olazabal, A., Santos Zalduegui, J.F., García de Madinabeitia, S., Tiepolo, M., Gil Ibarguchi, J.I., 2009. U-Pb dating of granodiorite and granite units of the Los Pedroches batholith. Implications for geodynamic models of the southern Central Iberian Zone (Iberian Massif). International Journal of Earth Sciences, 98, 1609–1624. http://dx.doi.org/10.1007/s00531-008-0317-0.
- Carrington da Costa, J., 1950. Noticia sobre uma carta geologica do Buçaco, de Nery Delgado. Lisboa, Publicación Especial de la Comision de Servicio Geológico de Portugal, 1–27.
- Castro, A., 1986. Structural pattern and ascent model in the Central Extremadura batholith, Hercynian belt, Spain. Journal of Structural Geology, 8(6), 633–645. https://doi.org/10.1016/0191-8141(86)90069-6.
- Castro, A., 2014. The off-crust origin of granite batholiths. Geoscience Frontiers, 5, 63–75. http://dx.doi.org/10.1016/j.gsf.2013.06.006.
- Castro, A., Patiño-Douce, A., Corretgé, L.G., de la Rosa, J., El-Biad, M., El-Hmidi, H., 1999. Origin of peraluminous granites and granodiorites, Iberian Massif, Spain: an experimental test of granite petrogenesis. Contributions to Mineralogy and Petrology, 135(2), 255–276. http:// dx.doi.org/10.1007/s004100050511.
- Castro, A., Corretgé, L.G., de la Rosa, J., Enrique, P.,
 Martínez, F.J., Pascual, E., Lago, M., Arranz, E., Galé,
 C., Fernández, C., Donaire, T., López, S., 2002. Paleozoic
 Magmatism. In: Gibbons, W., Moreno, T. (eds.). The
 Geology of Spain, Geological Society, London, 117–153.
- Chicharro, E., Villaseca, C., Valverde-Vaquero, P., Belousova, E., López-García, J.A., 2014. Zircon U-Pb and Hf isotopic constraints on the genesis of a post-kinematic S-type Variscan tin granite: the Logrosán cupola (Central Iberian Zone). Journal of Iberian Geology 40(3), 451–470. http://dx.doi.org/10.5209/rev_JIGE.2014.v40.n3.43928.

- Corretgé, L.G., 1971. Estudio petrológico del Batolito de Cabeza de Araya (Cáceres). PhD Thesis, University of Salamanca, Spain, 453pp.
- Corretgé, L.G., 1983. Las rocas graníticas y granitoides del Macizo Ibérico. In: Comba, J.A. (ed.). Geología de España, Tomo 1, Instituto Geológico y Minero de España, Madrid, 569–592.
- Corretgé, L.G., Bea, F., Suárez, O., 1985. Las características geoquímicas del batolito de Cabeza de Araya (Cáceres, España). Implicaciones petrogenéticas. Trabajos de Geología Universidad de Oviedo, 15, 219–238.
- Corretgé, L.G., Castro, A., García-Moreno, O., 2004. Granitoides de la "serie mixta". In: Vera, J.A. (ed.). Geología de España. Madrid, Sociedad Geológica de España e Instituto Geológico y Minero de España, 115–116.
- Debon, F., Le Fort, P., 1983. A chemical-mineralogical classification of common plutonic rocks and associations. Transactions of the Royal Society of Edinburgh: Earth and Environmental Science, 73(3), 135–149. https://doi. org/10.1017/S0263593300010117.
- Dias, G., Leterrier, J., Mendes, A., Simoes, P., Bertrand, J., 1998.
 U-Pb zircon and monazite geochronology of post-collisional
 Hercynian granitoids from the Central Iberian Zone (Northern Portugal). Lithos, 45, 349–369. https://doi.org/10.1016/S0024-4937(98)00039-5.
- Fitton, J.G., James, D., Kempton, P.D., Ormerod, D.S., Leeman, W.P., 1988. The role of the lithospheric mantle in the generation of late Cenozoic basic magmas in the western United States. Journal of Petrology, Special Volume (1), 331–349. https://doi.org/10.1093/petrology/Special_Volume.1.331
- García de Madinabeitia, S., Santos Zalduegui, J.F., Gil Ibarguchi, J.I., Carracedo, M., 2003. Geocronologia del plutón de Campanario-La Haba (Badajoz) a partir del análisis de isótopos de Pb en circones y U-Th-Pb_{total} en monacitas. Geogaceta, 34, 27–30.
- García de Madinabeitia, S., Sánchez Lorda, M.E., Gil Ibarguchi, J.I., 2008. Simultaneous determination of major to ultratrace elements in geological samples by fusion-dissolution and inductively coupled plasma mass spectrometry techniques. Analytica Chimica Acta, 625(2), 117–130. http://dx.doi.org/10.1016/j.aca.2008.07.024.
- García-Moreno, O., 2004. Estudio experimental de las relaciones texturales y de fases en granitos peralumínicos de la "Serie Mixta" del Macizo Ibérico: El caso de Cabeza de Araya (Cáceres). PhD Thesis, University of Granada, Spain, 248pp.
- García-Moreno, O., Corretgé, L.G., Castro, A., 2007. Processes of assimilation in the genesis of cordierite leucomonzogranites from the Iberian massif: a short review. The Canadian Mineralogist, 45, 71–85. https://doi. org/10.2113/gscanmin.45.1.71.
- González Menéndez, L., 1998. Petrología y geoquímica del batolito granítico de Nisa-Alburquerque (Alto Alentejo, Portugal; Extremadura, España). PhD Thesis, University of Granada, Spain, 221pp.

- Gutiérrez-Alonso, G., Fernández-Suárez, J., Jeffries, T.E., Johnston, S.T., Pastor-Galán, D., Murphy, J.B., Franco, M.P., Gonzalo, J.C., 2011. Diachronous post-orogenic magmatism within a developing orocline in Iberia, European Variscides. Tectonics, 30(5), TC5008. https://doi.org/10.1029/2010TC002845.
- Harrison, T.M., Watson, E.B., 1984. The behavior of apatite during crustal anatexis: Equilibrium and kinetic considerations. Geochimica et Cosmochimica Acta, 48(7), 1467–1477. https://doi.org/10.1016/0016-7037(84)90403-4.
- Harrison, T.M., Watson, E.B., Aikman, A.B., 2007. Temperature spectra of zircon crystallization in plutonic rocks. Geology, 35(7), 635–638. https://doi.org/10.1130/G23505A.1.
- Jackson, S.E., Pearson, N.J., Griffin, W.L., Belousova, E.A., 2004. The application of laser ablation-inductively coupled plasma-mass spectrometry to in situ U–Pb zircon geochronology. Chemical Geology, 211(1–2), 47–69. https:// doi.org/10.1016/j.chemgeo.2004.06.017.
- Janoušek, V., 2006. Saturnin, R language script for application of accessory-mineral saturation models in igneous geochemistry. Geologica Carpathica, 57(2), 131–142.
- Janoušek, V., Farrow, C.M., Erban, V., 2006. Interpretation of Whole-rock Geochemical Data in Igneous Geochemistry: Introducing Geochemical Data Toolkit (GCDkit). Journal of Petrology, 47(6), 1255–1259. https://doi.org/10.1093/ petrology/egl013.
- Janoušek, V., Moyen, J.-F. Martin, H., Erban, V., Farrow, C., 2016. Geochemical Modelling of Igneous Processes–Principles And Recipes in R Language. Berlin, Springer-Verlag Berlin Heidelberg, 346pp. https://doi.org/10.1007/978-3-662-46792-3.
- Martínez Catalán, J.R., Arenas, R., Abati, J., Sánchez Martínez, S., Díaz García, F., Fernández Suárez, J., González Cuadra, P., Castiñeiras, P., Gómez Barreiro, J., Díez Montes, A., González Clavijo, E., Rubio Pascual, F.J., Andonaegui, P., Jeffries, T.E., Alcock, J.E., Díez Fernández, R., López Carmona, A., 2009. A rootless suture and the loss of the roots of a mountain chain: The Variscan belt of NW Iberia. Comptes Rendus Geoscience, 341, 114–126. https://doi.org/10.1016/j.crte.2008.11.004.
- Martínez Poyatos, D., Gutiérrez-Marco, J.C., Pardo Alonso, M.V., Rábano, I., Sarmiento, G., 2004. La secuencia paleozoica postcámbrica. In: Vera, J.A. (ed.). Geología de España. Sociedad Geológica de España e Instituto Geológico y Minero de España (SGE-IGME), Madrid, 81–83.
- McCulloch, M.T., Chappell, B.W., 1982. Nd isotopic characteristics of S- and I-type granites. Earth and Planetary Science Letters, 58(1), 51–64. http://dx.doi.org/10.1016/0012-821X(82)90102-9.
- Meinhold, G., Kostopoulos, D., Frei, D., Himmerkus, F., Reischmann, T., 2010. U-Pb LA-SF-ICP-MS zircon geochronology of the Serbo-Macedonian Massif, Greece: palaeotectonic constraints for Gondwana-derived terranes in the Eastern Mediterranean. International Journal of Earth Sciences (Geologische Rundschau), 99(4), 813–832. https:// doi.org/10.1007/s00531-009-0425-5.

- Merino Martínez, E., Villaseca, C., Orejana, D., Pérez-Soba, C.,
 Belousova, E., Andersen, T., 2014. Tracing magma sources of three different S-type peraluminous granitoid series by in situ U-Pb geochronology and Hf isotope zircon composition:
 The Variscan Montes de Toledo batholith (central Spain).
 Lithos, 200–201, 273–298. http://dx.doi.org/10.1016/j. lithos.2014.04.013.
- Miller, C.F., Stoddard, E.F., Bradfish, L.J., Dollase, W.A., 1981. Composition of plutonic muscovite: genetic implications. The Canadian Mineralogist, 19, 25–34.
- Miller, C.F., McDowell, S.M., Mapes, R.W., 2003. Hot and cold granites? Implications of zircon saturation temperatures and preservation of inheritance. Geology, 31(6), 529–532. http://dx.doi.org/10.1130/0091-7613(2003)031<0529:HACGIO>2. 0.CO;2.
- Montel, J.-M., 1993. A model for monazite/melt equilibrium and application to the generation of granitic magmas. Chemical Geology, 110(1–3), 127–146. http://dx.doi.org/10.1016/0009-2541(93)90250-M.
- Montel, J.-M., Vielzeuf, D., 1997. Partial melting of metagreywackes, Part II. Composition of minerals and melts. Contributions to Mineralogy and Petrology, 128(2), 176–196. https://doi.org/10.1007/s004100050302.
- Montero, P., Bea, F., González-Lodeiro, F., Talavera, C., Whitehouse, M., 2007. Zircon crystallization age and protolith history of the metavolcanic rocks and metagranites of the Ollo de Sapo Domain in central Spain. Implications for the Neoproterozoic to Early-Paleozoic evolution of Iberia. Geological Magazine, 144(6), 963–976. http://dx.doi.org/10.1017/S0016756807003858.
- Montero, P., Talavera, C., Bea, F., Lodeiro, F.G., Whitehouse, M.J., 2009. Zircon Geochronology of the Ollo de Sapo Formation and the Age of the Cambro-Ordovician Rifting in Iberia. The Journal of Geology, 117, 174–191. https://doi. org/10.1086/595017.
- Nachit, H., Razafimahefa, N., Stussi, J.-M., Carron, P.J., 1985. Composition chimique des biotites et typologie magmatique des granitoïdes. Comptes Rendus de l'Académie des Sciences, 301(11), 813–818.
- Nachit, H., Ibhi, A., Abia, E.H., Ohoud, M.B., 2005. Discrimination between primary magmatic biotites, reequilibrated biotites and neoformed biotites. Comptes Rendus Geoscience, 337(16), 1415–1420. http://dx.doi.org/10.1016/j.crte.2005.09.002.
- O'Connor, J.T., 1965. A classification for quartz-rich igneous rocks based on feldspar ratios. In: Nolan, T.B. (ed.). U.S. Geological Survey, Professional Paper 525-B, 79–84.
- Orejana, D., Villaseca, C., Valverde-Vaquero, P., Belousova, E., Armstrong, A., 2012. U–Pb geochronology and zircon composition of late Variscan S- and I-type granitoids from the Spanish Central System batholith. International Journal of Earth Sciences (Geologische Rundschau), 101, 1789–1815.
- Patiño Douce, A.E., 1995. Experimental generation of hybrid silicic melts by reaction of high-Al basalt with metamorphic rocks. Journal of Geophysical Research, 100(B8), 15623–15639. https://doi.org/10.1029/94JB03376.

- Patiño Douce, A.E., Johnston, A.D., 1991. Phase equilibria and melt productivity in the pelitic system: implications for the origin of peraluminous granitoids and aluminous granulites. Contributions to Mineralogy and Petrology, 107(2), 202– 218. https://doi.org/10.1007/BF00310707.
- Patiño Douce, A.E., Humphreys, E.D., Johnston, A.D., 1990.

 Anatexis and metamorphism in tectonically thickened continental crust exemplified by the Sevier hinterland, western North America. Earth and Planetary Science Letters, 97(3–4), 290–315. https://doi.org/10.1016/0012-821X(90)90048-3.
- Paton, C., Hellstrom, J., Paul, B., Woodhead, J., Hergt, J., 2011. Iolite: Freeware for the visualisation and processing of mass spectrometric data. Journal of Analytical Atomic Spectrometry, 26, 2508–2518. https://doi.org/10.1039/ C1JA10172B.
- Petrus, J.A., Kamber, B.S., 2012. VizualAge: A Novel Approach to Laser Ablation ICP-MS U-Pb Geochronology Data Reduction. Geostandards and Geoanalytical Research, 36, 247–270. http://dx.doi.org/10.1111/j.1751-908X.2012.00158.x.
- Pichavant, M., Montel, J-M., Richard, L.R., 1992. Apatite solubility in peraluminous liquids: Experimental data and an extension of the Harrison-Watson model. Geochimica et Cosmochimica Acta, 56(10), 3855–3861. http://dx.doi.org/10.1016/0016-7037(92)90178-L.
- Rapp, R.P., Watson, E.B., 1986. Monazite solubility and dissolution kinetics: implications for the thorium and light rare earth chemistry of felsic magmas. Contributions to Mineralogy and Petrology, 94(3), 304–316. http://dx.doi. org/10.1007/BF00371439.
- Rodríguez Alonso, M.D., Díez Balda, M.A., Perejón, A., Pieren, A., Liñan, E., López Díaz, F., Moreno, F., Gámez Vintaned, J.A., González Lodeiro, F., Martínez Poyatos, D., Vegas, R., 2004. La secuencia litoestratigráfica del Neoproterozoico-Cámbrico Inferior. In: Vera, J.A. (ed.). Geología de España, Sociedad Geológica de España e Instituto Geológico y Minero de España (SGE-IGME), Madrid, 78–81.
- Rossi, P., Chevremont, P., 1987. Classification des associations magmatiques granitoides. Géochronique, 21, 14–18.
- Rudnick, R.L., Gao, S., 2003. Composition of the continental crust. In: Holland, H.D., Turekian, K.K. (eds.). Treatise on Geochemistry. Oxford, Elsevier-Pergamon, 1–64.
- Saunders, A.D., Norry, M.J., Tarney, J., 1988. Origin of MORB and Chemically-Depleted Mantle Reservoirs: Trace Element Constraints. Journal of Petrology, Special Volume (1), 415–445. http://dx.doi.org/10.1093/petrology/Special_ Volume.1.415.
- Sláma, J., Kosler, J., Condon, D.J., Crowley, J.L., Gerdes, A., Hanchar, J.M., Horstwood, M.S.A., Morris, G.A., Nasdala, L., Norberg, N., Schaltegger, U., Schoene, B., Tubrett, M.N., Whitehouse, M.J., 2008. Plešovice zircon - a new natural reference material for U–Pb and Hf isotopic microanalysis. Chemical Geology, 249, 1–35. https://doi.org/10.1016/j. chemgeo.2007.11.005.

- Solá, A.R., Williams, I.S., Neiva, A.M.R., Ribeiro, M.L., 2009. U-Th-Pb SHRIMP ages and oxygen isotope composition of zircon from two contrasting late Variscan granitoids, Nisa-Albuquerque batholith, SW Iberian Massif: Petrologic and regional implications. Lithos, 111(3–4), 156–167. http://dx.doi. org/10.1016/j.lithos.2009.03.045.
- Sun, S.S., McDonough, W.F., 1989. Chemical and isotopic systematics of oceanic basalts; implications for mantle composition and processes. In: Saunders, A.D., Norry, M.J. (eds.). Magmatism in the ocean basins. London, Geological Society of London, 42 (Special Paper), 313–345.
- Sylvester, J.P., 1998. Post-collisional strongly peraluminous granites. Lithos, 45(1–4), 29–44. http://dx.doi.org/10.1016/ S0024-4937(98)00024-3.
- Talavera, C., Bea, F., Montero, P., Whitehouse, M., 2008. A revised Ordovician age for the Sisargas orthogneiss, Galicia (Spain). Zircon U-Pb ion-microprobe and LA-ICPMS dating. Geologica Acta, 6(4), 313–317. http://dx.doi.org/10.1344/105.000000259.
- Talavera, C., Montero, P., Martínez Poyatos, D., Williams, I.S., 2012. Ediacaran to Lower Ordovician age for rocks ascribed to the Schist-Greywacke Complex (Iberian Massif, Spain): Evidence from detrital zircon SHRIMP U-Pb geochronology. Gondwana Research, 22(3–4), 928–942. http://dx.doi. org/10.1016/j.gr.2012.03.008.
- Talavera, C., Montero, P., Bea, F., González Lodeiro, F., Whitehouse, M., 2013. U-Pb Zircon geochronology of the Cambro-Ordovician metagranites and metavolcanic rocks of central and NW Iberia. International Journal of Earth Sciences (Geologische Runschau), 102, 1–23. https://doi.org/10.1007/ s00531-012-0788-x.
- Villaseca, C., Barbero, L., Herreros, V., 1998a. A re-examination of the typology of peraluminous granite types in intracontinental orogenic belts. Earth and Environmental Science Transactions of The Royal Society of Edinburgh, 89(2), 113–119. https:// doi.org/10.1017/S0263593300007045.
- Villaseca, C., Barbero, L., Rogers, G., 1998b. Crustal origin of Hercynian peraluminous granitic batholiths of Central Spain: petrological, geochemical and isotopic (Sr, Nd) constraints. Lithos, 43(2), 55–79. https://doi.org/10.1016/S0024-4937(98)00002-4.
- Villaseca, C., Downes, H., Pin, C., Barbero, L., 1999. Nature and Composition of the Lower Continental Crust in Central Spain and the Granulite–Granite Linkage: Inferences from Granulitic Xenoliths. Journal of Petrology, 40(10), 1465–1496. https://doi.org/10.1093/petroj/40.10.1465.
- Villaseca, C., Pérez-Soba, C., Merino, E., Orejana, D., López-García, J.A., Billstrom, K., 2008. Contrasting crustal sources for peraluminous granites of the segmented Montes de Toledo batholith (Iberian Variscan Belt). Journal of Geosciences, 53, 263–280.
- Villaseca, C., Orejana, D., Beolousova, A.E., 2012. Recycled metaigneous crustal sources for S- and I-type Variscan granitoids from the Spanish Central System batholith: Constraints from Hf isotope zircon composition. Lithos, 153, 84–93. https://doi.org/10.1016/j.lithos.2012.03.024.

Villaseca, C., Merino Martínez, E., Orejana, D., Andersen, T., Beolousova, E., 2016. Zirzon Hf signatures from granitic orthogneisses of the Spanish Central System: Significance and sources of the Cambro-Ordovician magmatism in the Iberian Variscan Belt. Gondwana Research, 34, 60–83. http:// dx.doi.org/10.1016/j.gr.2016.03.004. Watson, E.B., Harrison, T.M., 1983. Zircon saturation revisited: temperature and composition effects in a variety of crustal magma types. Earth and Planetary Science Letters, 64(2), 295–304. http://dx.doi.org/10.1016/0012-821X(83)90211-X
Wilson, M., 1989. Igneous Petrogenesis: a Global Tectonic Approach. London, Unwin Hyman, 466pp.

Manuscript received January 2017; revision accepted November 2017; published Online November 2017.